*I.J. Intelligent Systems and Applications,* **2013, 09, 76-85**
Published Online August 2013 in MECS (http://www.mecs-press.org/)
DOI: 10.5815/ijisa.2013.09.09

# Non-isothermal Flow through a Curved Channel with Strong Curvature

**M. M. Rahman***
Department of Mathematics, Islamic University, Kushita-7003, Bangladesh
*E-mail**: *mizan_iu@yahoo.com*

**M. A. Hye**
Department of Mathematics & Statistics, Bangladesh University of Business & Technology, Dhaka-1216, Bangladesh

***Abstract*—** Non-isothermal flow through a curved square channel with strong curvature is investigated numerically by using the spectral method and covering a wide range of the Dean number, Dn, $100 \le Dn \le 6000$ for the curvature $\delta = 0.5$ . A temperature difference is applied across the vertical sidewalls for the Grashof number $Gr = 100$, where the outer wall is heated and the inner one cooled. After a compressive survey over the parametric ranges, two branches of asymmetric steady solutions with two- and four-vortex solutions are obtained by the Newton-Raphson iteration method. Then, in order to investigate the non-linear behavior of the unsteady solutions, time evolution calculations as well as power spectrum of the solutions are obtained, and it is found that in the unsteady flow undergoes in the scenario "*steady* $\rightarrow$ *periodic* $\rightarrow$ *multi-periodic* $\rightarrow$ *chaotic*", if *Dn* is increased.

***Index Terms*—** Curved Duct, Dean Number, Secondary Flow, Curvature, Time Evolution

## I. Introduction

The study of flows and heat transfer through curved ducts and channels has been and continues to be an area of paramount interest of many researchers because of the diversity of their practical applications in fluids engineering, such as in fluid transportation, turbo machinery, refrigeration, air conditioning systems, heat exchangers, ventilators, centrifugal pumps, internal combustion engines and blade-to-blade passage for cooling system in modern gas turbines. Blood flow in the human and other animals also represents an important application of this subject because of the curvature of many blood vessels, particularly the aorta. The flow through curved a duct shows physically interesting features under the action of centrifugal force caused by the curvature of the duct. The presence of curvature produces centrifugal forces which acts at right angle to the main flow direction and creates secondary flows. Dean (1927) was the first who formulated the problem in mathematical terms under the fully developed flow conditions and showed the existence of a pair of counter rotating vortices in a curved pipe. In consideration of the importance, flows in curved ducts have been studied extensively in the literature for several decades, the readers are referred to Berger *et al*. (1983), Nandakumar and Masliyah (1986), Ito (1987) and Yanase *et al*. (2002) for some outstanding reviews on curved duct flows.

The non-linear nature of the Navier-Stokes equation, the existence of multiple solutions does not come as a surprise. The solution structure of fully developed flow is commonly present in a bifurcation diagram which consists of a number of lines (branches) connecting different possible solutions. These branches can bifurcate and show multiple solutions in limit points (Mondal, 2006). An early complete bifurcation study of two-dimensional (2-D) flow through a curved duct of square cross section was conducted by Winters (1987). Very recently, Mondal *et al*. (2007a) performed comprehensive numerical study on fully developed bifurcation structure and stability of two-dimensional (2D) flow through a curved duct with square cross section and found a close relationship between the unsteady solutions and the bifurcation diagram of steady solutions. The flow through a curved duct with differentially heated vertical sidewalls has another aspect because secondary flows promote fluid mixing and heat transfer in the fluid (Yanase *et al*., 2005). They also studied the transitional behavior of the unsteady solutions by time evolution calculations.

Many researchers have performed experimental and numerical investigation on developing and fully developed curved duct flows. An early complete bifurcation study of two-dimensional (2-D) flow through a curved duct with square cross section was performed by Winters (1987). Our ultimate goal is to investigate the non-isothermal flows through a curved channel with the presence of buoyancy effects by considering the strong curvature. Mondal et al. (2006) performed numerical prediction of non-isothermal flow through a curved square duct over a wide range of the curvature and the Dean number. They showed that

 

stability characteristics drastically change due to an increase of curvature. However, there has not yet been done any substantial work regarding the flow characteristics through a curved square duct for large curvature ; this paper is, therefore, an attempt to fill up this gap with the investigation of the flow characteristics through a curved square channel for strong curvature because this type of flow is often encountered in engineering applications. From the scientific as well as engineering point of view, it is quite interesting to study curved channel flows with differentially heated vertical sidewalls for the large Grashof number, because this type of flow is often encountered in engineering applications. The present study is, therefore, an attempt to fill up this gap with the study of the non-linear behavior of the unsteady solutions by time-evolution calculation.

In the present paper, a numerical study is presented for the fully developed two-dimensional flow of viscous incompressible fluid through a curved square channel with differentially heated vertical sidewalls. Flow characteristics are studied over a wide range of the Dean number and the strong curvature by finding the steady solutions, investigating their linear stability and analyzing nonlinear behavior of the unsteady solutions by time evolution calculations.

## II. Governing Equations

Consider a hydro dynamically and thermally fully developed two-dimensional flow of viscous incompressible fluid through a curved duct with square cross section. Let $2d$ be the width of the cross section. The coordinate system with the relevant notations is shown in Fig 1. Where *C* is the centre of the curvature and *L* is the radius of the curvature. Let $x$ and $y$ axes are taken to be in the horizontal and vertical directions respectively, and $z$ is the coordinate along the center-line of the duct, i.e., the axial direction. It is assumed that the outer wall of the duct is heated while the inner one is cooled. The temperature of the outer wall is $T_0 + \Delta T$ and that of the inner wall is $T_0 - \Delta T$, where $\Delta T > 0$.

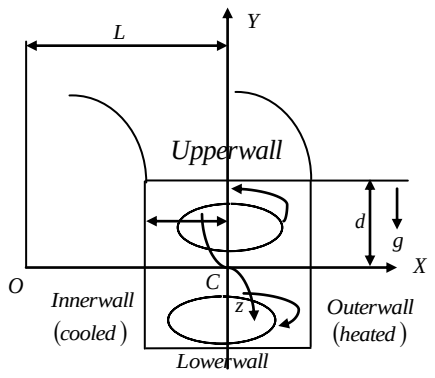


Fig. 1: Coordinate system of the curved square duct

It is also assumed that the flow is uniform in the axial direction, and that it is driven by a constant pressure gradient $G\left(G = -\frac{\partial P'}{\partial z'}\right)$ along the center-line of the duct. The main flow in the $z$ direction as in Fig. 1.

The dimensional variables are then non-dimensional zed by using the representative length $l$, the representative velocity $U_0 = \frac{\upsilon}{d}$, where $\upsilon$ is the kinematic viscosity of the fluid. We introduce the non-dimensional variables defined as

$$u = \frac{u'}{U_0},\ v = \frac{v'}{U_0},\ w = \frac{\sqrt{2\delta}}{\mathrm{U_o}} w',$$

$$x = \frac{x'}{d}, \qquad \bar{y} = \frac{y'}{d}, \qquad z = \frac{z'}{d}$$

$$T = \frac{T'}{\Delta T'},\ t = \frac{U_0}{d} t', \quad \delta = \frac{d}{L},$$

$$P = \frac{P'}{\rho {U_0}^2}, \quad G = -\frac{\partial P'}{\partial z'} \frac{d}{\rho U_0^2}$$

where $u, v$ and $w$ are the non-dimensional velocity components in the $x, y$ and $z$ directions, respectively; $t$ is the non-dimensional time, $P$ is the non-dimensional pressure, $\delta$ is the non-dimensional curvature defined as $\delta = \frac{d}{L}$, and temperature is non-dimensional zed by $\Delta T$. Hence forth, all the variables are non-dimensional zed if not specified.

Since the flow field is uniform in the $z$ direction, the sectional stream function $\psi$ is introduced as

$$u = \frac{1}{1+\delta x} \frac{\partial \psi}{\partial \bar{y}}, \quad v = -\frac{1}{1+\delta x} \frac{\partial \psi}{\partial x} \tag{1}$$

A new coordinate variable y is introduced in the $\bar{y}$ direction as $\bar{y} = a\, y$, where $a = \frac{h}{l}$ is the aspect ratio of the duct cross section. In this study, we consider the case for $h = l$ i.e. $a = 1$ (square duct). Then, the basic equations for $w, \psi$ and $T$ are expressed in terms of non-dimensional variables as

$$(1+\delta x)\frac{\partial w}{\partial t} + \frac{\partial (w,\psi)}{\partial (x,y)} - Dn + \frac{\delta^2 w}{1+\delta x} =$$
$$(1+\delta x)\Delta_2 w - \frac{\delta}{1+\delta x}\frac{\partial \psi}{\partial y} w + \delta \frac{\partial w}{\partial x} \tag{2}$$

$$\left(\Delta_2-\frac{\delta}{1+\delta x}\frac{\partial}{\partial x}\right)\frac{\partial\psi}{\partial t}=$$
$$-\frac{1}{(1+\delta x)}\frac{\partial(\Delta_2\psi,\psi)}{\partial(x,y)}$$
$$+\frac{\delta}{(1+\delta x)^2}\left[\begin{array}{l}\frac{\partial\psi}{\partial y}\left(2\Delta_2\psi-\frac{3\delta}{1+\delta x}\frac{\partial\psi}{\partial x}+\frac{\partial^2\psi}{\partial x^2}\right)\\ -\frac{\partial\psi}{\partial x}\frac{\partial^2\psi}{\partial x\partial y}\end{array}\right]$$
$$+\frac{\delta}{(1+\delta x)^2}\times\left[3\delta\frac{\partial^2\psi}{\partial x^2}-\frac{3\delta^2}{1+\delta x}\frac{\partial\psi}{\partial x}\right] \quad (3)$$
$$-\frac{2\delta}{1+\delta x}\frac{\partial}{\partial x}\Delta_2\psi$$
$$+w\frac{\partial w}{\partial y}$$
$$+{\Delta_2}^2\psi-Gr(1+\delta x)\frac{\partial T}{\partial x}$$

$$\frac{\partial T}{\partial t}+\frac{1}{(1+\delta x)}\frac{\partial(T,\psi)}{\partial(x,y)}=$$
$$\frac{1}{\Pr}\left(\Delta_2 T+\frac{\delta}{1+\delta x}\frac{\partial T}{\partial x}\right) \quad (4)$$

where,

$$\Delta_2\equiv\frac{\partial^2}{\partial x^2}+\frac{\partial^2}{\partial y^2},$$
$$\frac{\partial(T,\psi)}{\partial(x,y)}\equiv\frac{\partial f}{\partial x}\frac{\partial g}{\partial y}-\frac{\partial f}{\partial y}\frac{\partial g}{\partial x} \quad (5)$$

The non-dimensional parameters $Dn$, the Dean number, $Gr$, the Grashof number, and $\Pr$, the prandtl number, which appear in equation (2) - (4) are defined as

$$Dn=\frac{Gd^3}{\mu\upsilon}\sqrt{\frac{2d}{L}}$$
$$Gr=\frac{\beta g\Delta T\,d^3}{\upsilon^2},\quad \Pr=\frac{\upsilon}{\kappa} \quad (6)$$

Where $\mu$, $\beta,\kappa$ and $g$ are the viscosity, the coefficient of thermal expansion, the co-efficient of thermal diffusivity and the gravitational acceleration respectively is the viscosity of the fluid. In the present study, only $Dn$ is varied while $\delta$, $Gr$ and Pr are fixed as $\delta=0.5$, $Gr=100$ and $\Pr=7.0$ (water). The rigid boundary conditions used here for $w$ and $\psi$ are

$$w(\pm1,y)=w(x,\pm1)=\psi(\pm1,y)=\psi(x,\pm1)$$
$$=\frac{\partial\psi}{\partial x}(\pm1,y)=\frac{\partial\psi}{\partial y}(x,\pm1)=0 \quad (7)$$

and the temperature $T$ is assumed to be constant on the walls as

$$T(1,y)=1,\ T(-1,y)=-1,T(x,\pm1)=x \quad (8)$$

It should be noted that the Equations (2), (3) & (4) are invariant under the transformation of the variables

$$\left.\begin{array}{l}y\Rightarrow-y\\ w(x,y,t)\Rightarrow w(x,-y,t),\\ \psi(x,y,t)\Rightarrow-\psi(x,-y,t),\\ T(x,y,t)\Rightarrow-T(x,-y,t)\end{array}\right\} \quad (9)$$

Therefore, the case of heating the inner sidewall and cooling the outer sidewall can be deduced directly from the results obtained in this study. Equations (2) – (4) would serve as the basic governing equations which will be solved numerically as discussed in the following section.

## III. Numerical Calculations

The present study is based on numerical calculations to solve the equation (2)-(4), the spectral method is used. This is the method which is thought to be the best numerical method for solving the Navier-Stokes as well as energy equations (Gottlieb and Orszag, 1997). By this method the variables are expanded in a series of functions consisting of Chebyshev polynomials. The expansion functions $\phi_n(x)$ and $\psi_n(x)$ are expressed as

$$\left.\begin{array}{l}\phi_n(x)=(1-x^2)C_n(x),\\ \psi_n(x)=(1-x^2)^2C_n(x)\end{array}\right\} \quad (10)$$

where $C_n(x)=\cos\left(n\cos^{-1}(x)\right)$ is the $n^{th}$ order Chebyshev polynomial. $w(x,y,t)$, $\psi(x,y,t)$ and $T(x,y,t)$ are expanded in terms of the expansion functions $\phi_n(x)$ and $\psi_n(x)$ as:

$$w(x,y,t)=\sum_{m=0}^{M}\sum_{n=0}^{N}w_{mn}(t)\times\varphi_m(x)\varphi_n(y)$$
$$\psi(x,y,t)=\sum_{m=0}^{M}\sum_{n=0}^{N}\psi_{mn}(t)\times\psi_m(x)\psi_n(y) \quad (11)$$
$$T(x,,y,t)=\sum_{m=0}^{M}\sum_{n=0}^{N}T_{mn}\times\varphi_m(x)\varphi_n(y)$$

 

where $M$ and $N$ are the truncation numbers in the $x$ and $y$ directions respectively .

The collocation points $(x_i, y_j)$ are taken to be

$$\left.\begin{aligned} x_i &= \cos\left[\pi\left(1-\frac{i}{M+2}\right)\right], \qquad i=1,\ldots,M+1 \\ y_j &= \cos\left[\pi\left(1-\frac{j}{N+2}\right)\right], \qquad j=1,\ldots,N+1 \end{aligned}\right\} \quad (12)$$

where $i=1,\ldots,M+1$ and $j=1,\ldots,N+1$ . Steady solutions are obtained by the Newton-Rapshon iteration method assuming that all the variables are time independent. The convergence is assured by taking sufficiently small $\varepsilon_p$ ($\varepsilon_p < 10^{-10}$) defined as

$$\varepsilon_p = \sum_{m=0}^{M}\sum_{n=0}^{N}\left[\begin{aligned}&\left(w_{mn}^{(p+1)}-w_{mn}^{p}\right)^2+\left(\psi_{mn}^{(p+1)}-\psi_{mn}^{p}\right)^2 \\ &+\left(T_{mn}^{(p+1)}-T_{mn}^{p}\right)^2\end{aligned}\right]. \quad (13)$$

The present numerical calculation, for sufficiently accuracy of the solutions, we take $M=20$ and $N=20$ for a square duct. Finally, in order to calculate the unsteady solutions, the Crank-Nicolson and Adams-Bashforth methods together with the function expansion (11) and the collocation methods are applied to equations (2)-(4).

## IV. Time-evolution Calculation

In order to solve the non-linear time evolution equations, we use the Crank-Nicolson and Adams-Bashforth method. For the Crank-Nicolson method more explicitly, we consider the following one-dimensional heat-flow equation

$$\frac{\partial q}{\partial t} = \sigma\frac{\partial^2 q}{\partial x^2} \quad (14)$$

where $q(t)$ the temperature is at time $t$ regarded as a function of $x$ and $\sigma$ is the heat conductivity. The first time derivative in Esq. (14) is replaced by a finite difference ratio and a time step $\Delta t$ , the derivative with respect to time may be written as

$$\frac{\partial q}{\partial t} \approx \frac{q(t+\Delta t)-q(t)}{\Delta t} \text{ as } \Delta t \to 0$$

Now taking the average at $t$ and $t+1$ , Esq. (14) becomes approximately,

$$\frac{q(t+\Delta t)-q(t)}{\Delta t} = \frac{\sigma}{2}\frac{\partial^2}{\partial x^2}[q(t+\Delta t)-q(t)] \quad (15)$$

The approximate solution of Eq. (14), thus evaluated, is a function of $\Delta t$ as well as $x$ and $t$ , and the true solution is the limit of the approximate one as $\Delta t \to 0$ . The method, determined by Eq. (15), is called the Crank-Nicolson method. The Adams-Bashforth Method, on the other hand, is used for numerically solving initial value problems for ordinary differential equations. This method is an explicit linear multistep method that depends on multistep previous solution points to generate a new approximate solution point.

## V. Results and Discussion

In this study, we have investigated time evolution of the resistance coefficients $\lambda$ for the non-isothermal flows through a curved square channel with strong curvature $\delta = 0.5$ . We have studied the steady and unsteady solutions of the flows at various Dean numbers, $Dn$ , $100 \le Dn \le 6000$ for a fixed Grashof number $Gr = 100$ . In addition to the time evaluation of $\lambda$ , the secondary flow patterns, axial flow distributions and temperature profiles at various Dean numbers are discussed in detail.

### 5.1 Steady Solution

With the present numerical calculation, we obtain two branches of steady solutions for $Gr = 100$ over the Dean number $0 \le Dn \le 3000$ by using the path continuation technique as discussed in Keller (1987). The two steady solution branches are named the ***first steady solution branch*** (first branch, bold solid line) and the ***second steady solution branch*** (second branch, thin solid line), respectively. Fig. 2 shows solution structure of the steady solutions for the flow through a curved square channel with strong curvature. It is found that there exists no bifurcating relationship between the two branches of steady solutions as shown in Fig. 2. In the following, the two steady solution branches as well as the flow patterns and temperature profiles on the respective branches are discussed.

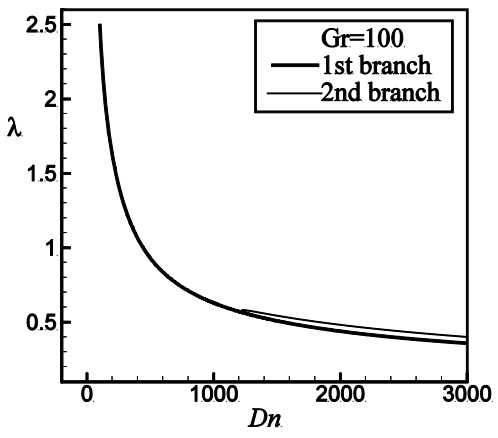


Fig. 2: Steady solution branches for curvature $\delta = 0.5$ for $Gr = 100$

### 5.2 Unsteady Solutions:

**Time evolution of the unsteady solutions for** $Dn \le 4345$

We performed time evolution of the resistance coefficient $\lambda$ for $Dn \le 4345$ at $Gr = 100$, and it is found that the flow is steady-state for all the values of $Dn$ in this range. Fig. 3(a) shows time evolution of $\lambda$ for $Dn = 4345$. Typical contours of secondary flow, axial flow distribution and temperature profiles for at $Dn = 4345$ are shown in the Fig. 3(b). As seen in Fig. 3(b), the secondary flow is two-vortex solutions for the steady-state solution. If the Dean number is increased a little for example $Dn = 4350$, the steady flow turns into periodic solution. It is found that the transition from steady-state solution to periodic oscillation occurs for $\delta = 0.5$ between $Dn = 4345$ and $Dn = 4350$.

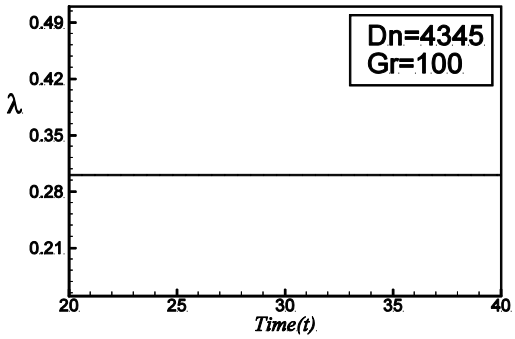


(a)

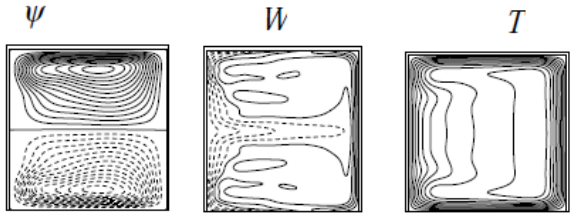


(b)

Fig. 3: **(a)** Time evolution of $\lambda$ for $Dn = 4345$ and $Gr = 100$ at time $20 \le t \le 40$ for the large curvature $\delta = 0.5$ ; **(b)** Contours of secondary flow, axial flow distribution and temperature profile for $Dn = 4345$ at time $t = 25$

**Time evolution of the unsteady solutions for** $4350 \le Dn \le 4475$

We studied the time evolution of the resistance coefficient $\lambda$ for $4350 \le Dn \le 4440$. It is found that the flow is periodic for all the values of $Dn$ in the above range. Fig. 4(a) and Fig. 5(a) show that the flow is periodic oscillations for $Dn = 4350$ and $Dn = 4440$. In order to investigate the periodic behavior more clearly, power spectrum of the time evaluation for $Dn = 4350$ and $Dn = 4440$ are shown in Fig. 4(b) and 5(b) respectively, where the line spectra of the fundamental frequency and its harmonics are seen, which suggests that the flow is periodic for both the cases. Typical contours of secondary flow; axial flow distribution and temperature profiles are shown in Fig. 4(c) for $Dn = 4350$ and in Fig. 5(c) for $Dn = 4440$ for one period of oscillation at time $76.80 \le t \le 76.88$ and $37.355 \le t \le 37.430$. As seen in Fig. 4(c) and 5(c), the secondary flow is a two -vortex solutions for both $Dn = 4350$ and $Dn$ = 4440. Next we investigate time evolution of $\lambda$ for $Dn = 4475$ as shown in Fig. 6(a). It is found that the flow oscillates multi-periodically. Then to justify whether the flow is periodic or multi-periodic, we plot the power spectrum of the time change of $\lambda$ at $Dn = 4475$ in Fig. 6(b), where it is seen that only the line spectrum of the fundamental frequency and its harmonic are available but no other line spectrum with smaller frequencies are seen, which suggests that the flow is periodic but not multi-periodic. Then typical contours of secondary flow patterns; axial flow distribution and temperature profiles are shown in Fig. 6(c) for $Dn = 4475$, one period of oscillation at time $21.60 \le t \le 21.67$. As seen in Fig. 6(c), the secondary flow is two -vortex solution for $Dn = 4475$. Thus it is seen that the periodic oscillations from $Dn = 4350$ to $Dn = 4475$ oscillates between two-vortex solution. If the Dean number is increased further, for example $Dn = 5050$, the flow turns into multi-periodic. Thus the transition from periodic to multi-periodic oscillation occurs between $Dn = 4475$ and $Dn = 4500$

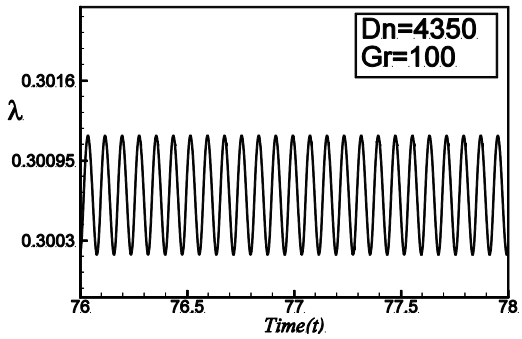


(a)

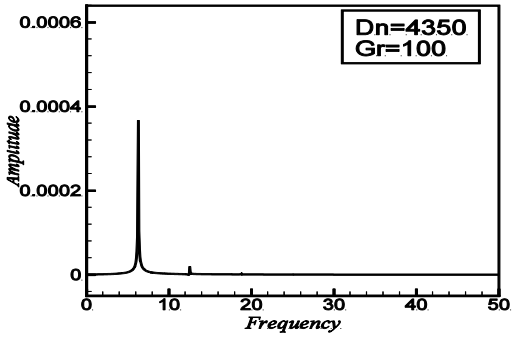


(b)

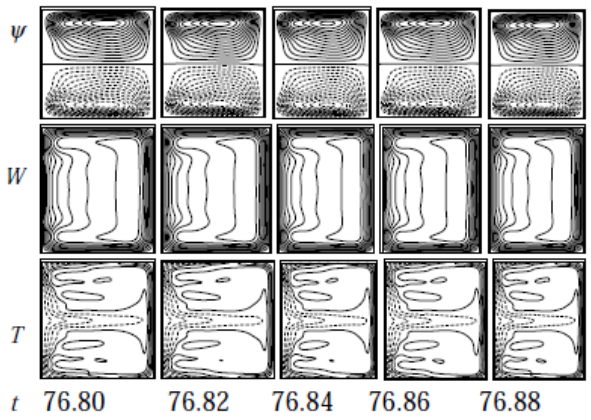


**(c)**

Fig. 4: **(a)** Time evolution of $\lambda$ for $Dn = 4350$ at time $76 \le t \le 78$ for $\delta = 0.5$ ; **(b)** Power spectra of the time evolution of $\lambda$ for $Dn = 4350$ for $\delta = 0.5$ **; (c)** Contours of secondary flow, axial flow distribution and temperature profiles for $Dn = 4350$ at time $76.80 \le t \le 76.88$

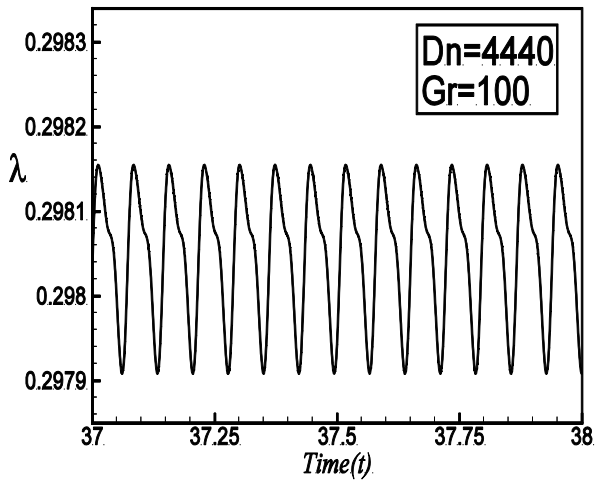


(a)

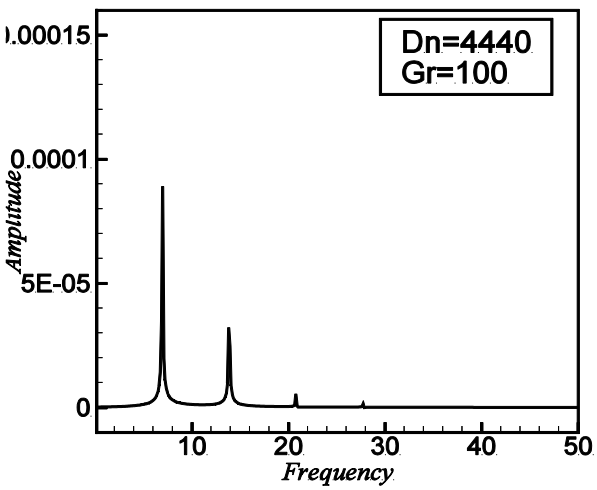


(b)

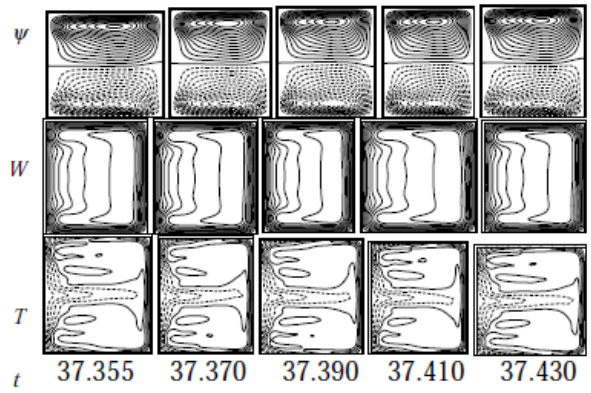


**(c)**

Fig. 5: **(a)** Time evolution of $\lambda$ for $Dn = 4440$ at time $37 \le t \le 38$ for $\delta = 0.5$ ; **(b)** Power spectra of the time evolution of $\lambda$ for $Dn = 4440$ for $\delta = 0.5$ ; **(c)** Contours of secondary flow, axial flow distribution and temperature profiles for $Dn = 4440$ at time $37.355 \le t \le 37.430$

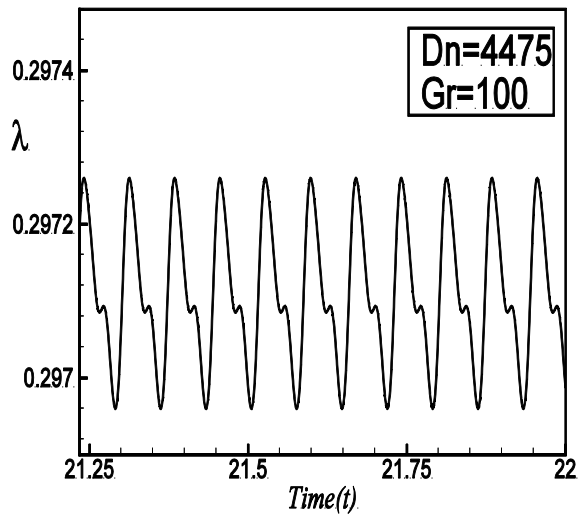


**(a)**

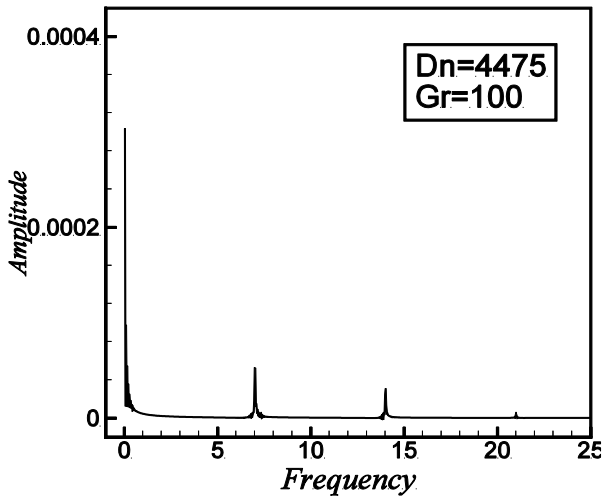


**(b)**

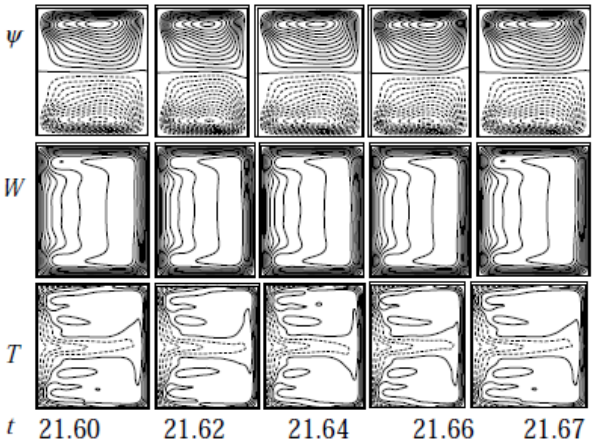


**(c)**

Fig. 6: **(a)** Time evolution of $\lambda$ for $Dn = 4475$ at time $21.25 \le t \le 22$ for $\delta = 0.5$ **; (b)** Power spectra of the time evolution of $\lambda$ for $Dn = 4475$ for $\delta = 0.5$ **; (c)** Contours of secondary flow, axial flow distribution and temperature profiles for $Dn = 4475$ at time $21.60 \le t \le 21.67$

**Time evolution of the unsteady solutions for** $4500 \le Dn \le 5050$

Next we investigate time evolution of $\lambda$ for $4500 \le Dn \le 5050$. It is found that the flow oscillates multi-periodically for $4500 \le Dn \le 5050$. Fig. 7(a) and 8(a) show the instance of multi-periodic oscillation for $Dn = 4500$ and $Dn = 5050$ respectively. In order to investigate the multi-periodic behavior more clearly, power spectrum of the time evaluation of $\lambda$ for $Dn = 5050$ is shown in Fig. 8(b), in which not only the line spectrum of the fundamental frequency and its harmonics but also other line spectrum and its harmonics are seen, which clearly suggests that the flow is multi-periodic. To observe that the change of the flow characteristics contours of typical secondary flow patterns, axial distribution and temperature profiles are shown in Fig. 7(b) for $Dn = 4500$ and in Fig. 8(c) for $Dn = 5050$ shown that one period of oscillation at time $9.490 \le t \le 9.565$ and $20.42 \le t \le 20.48$ respectively. As seen in Fig. 7(b) and 8(c), the secondary flow two-vortex solutions are found for both $Dn = 4500$ and $Dn = 5050$. If the Dean number is increased further, for example $Dn = 5075$, the flow turns into chaotic. It is found that the transition from multi-periodic to chaotic oscillation occurs between $Dn = 5050$ and $Dn = 5075$.

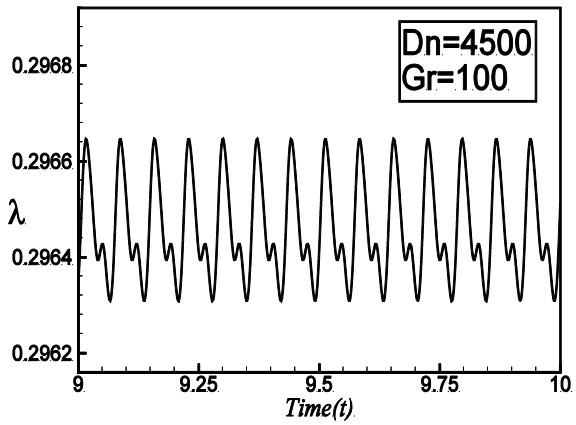


**(a)**

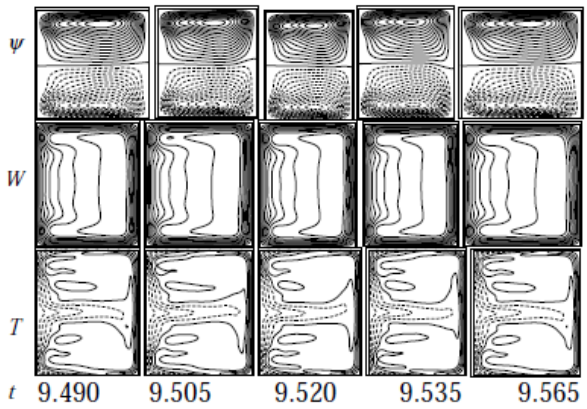


**(b)**

Fig. 7: **(a)** Time evolution of $\lambda$ for $Dn = 4500$ at time $9 \le t \le 10$ for $\delta = 0.5$ **; (b)** Contours of secondary flow, axial flow distribution and temperature profiles for $Dn = 4500$ at time $9.490 \le t \le 9.565$

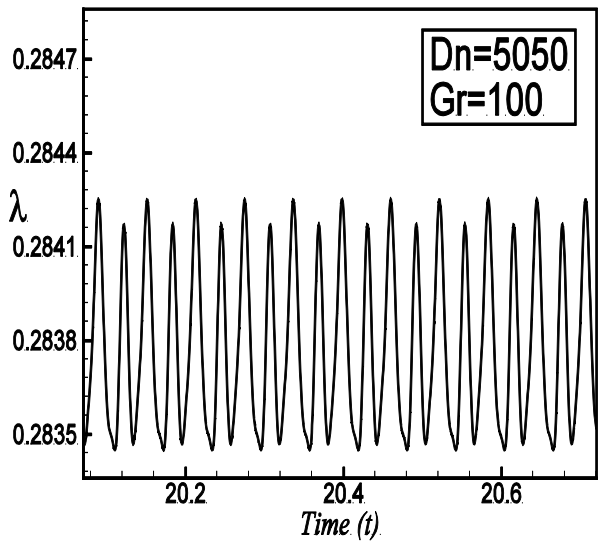


(a)

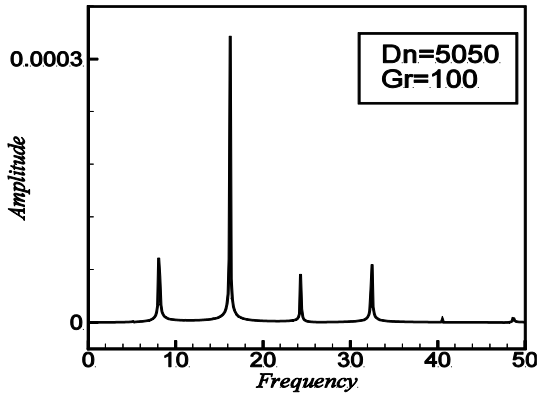


(b)

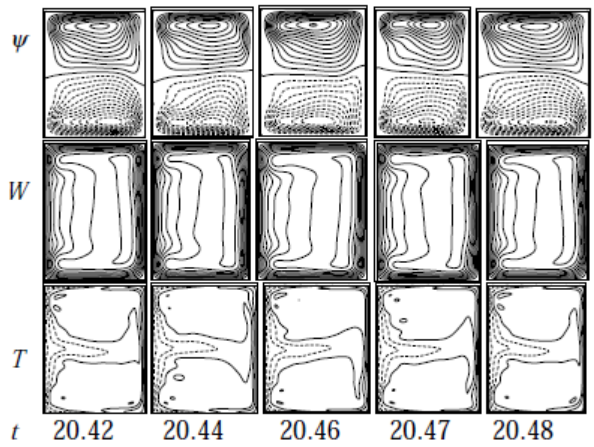


**(c)**

Fig. 8: **(a)** Time evolution of $\lambda$ for $Dn = 5050$ at time $20.08 \le t \le 20.72$ for $\delta = 0.5$ **; (b)** Power spectra of the time evolution of $\lambda$ for $Dn = 5050$ for $\delta = 0.5$ ; **(c)** Contours of secondary flow, axial flow distribution and temperature profiles for $Dn = 5050$ at time $20.42 \le t \le 20.48$

**Time evolution of the unsteady solutions for** $5075 \le Dn \le 5835$

We perform time evolution of $\lambda$ for $5075 \le Dn \le 5835$ . It is found that all the flow oscillates irregularly that is the flow is chaotic in this range. Fig. 9(a) and Fig. 10(a) show the instances of chaotic oscillations for $Dn = 5075$ and $Dn = 5835$ respectively. In order to investigate the chaotic behavior more clearly, power spectra of the time evaluation of $\lambda$ for $Dn = 5075$ and $Dn = 5835$ are shown in Fig. 9(b) and 10b) respectively. To observe that the change of the flow characteristics, contours of typical secondary flow patterns, axial distribution and temperature profiles are shown in Figure 9(c) and Fig. 10(c) for $Dn = 5075$ and $Dn = 5835$ respectively, where it is seen that the chaotic oscillation for $Dn = 5075$ and $Dn = 5835$ oscillates between asymmetric two-vortex solutions. Contours of secondary flow patterns, axial distribution and temperature profiles are shown in Fig. 9(c) for $Dn = 5075$ and one period of oscillation at time $45.00 \le t \le 45.40$ , and for $Dn = 5835$ one period of oscillation at time $20.00 \le t \le 20.40$ in Fig. 10(c). If the Dean number is increased further, for example $Dn = 5840$ , the flow turns into periodic. The transition from chaotic to periodic oscillation occurs between $Dn = 5835$ and $Dn = 5840$ .

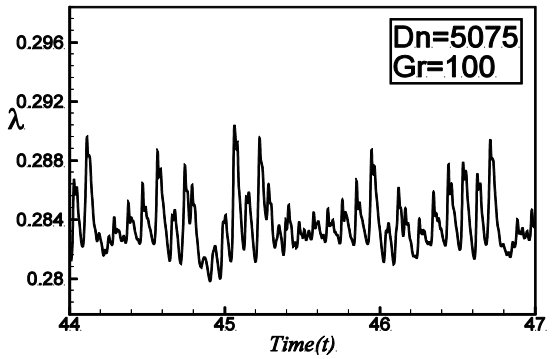


(a)

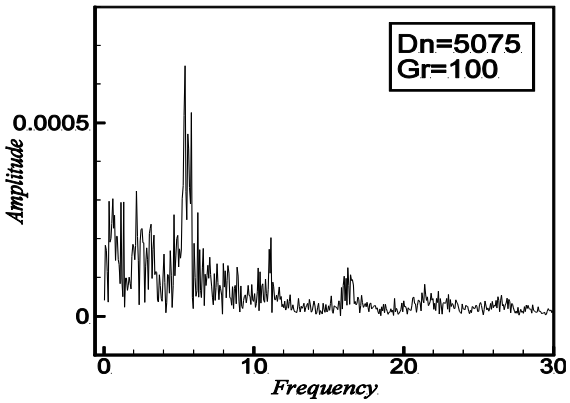


(b)

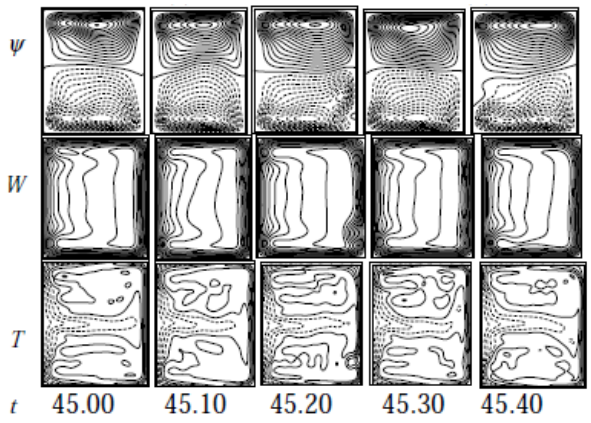


**(c)**

Fig. 9: **(a)** Time evolution of $\lambda$ for $Dn = 5075$ at time $44 \le t \le 47$ for $\delta = 0.5$ ; **(b)** Power spectra of the time evolution of $\lambda$ for $Dn = 5075$ for $\delta = 0.5$ **; (c)** Contours of secondary flow, axial flow distribution and temperature profiles for $Dn = 5075$ at time $45.00 \le t \le 45.40$

 

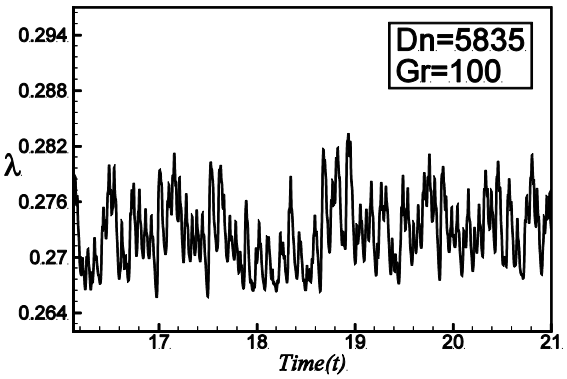


(a)

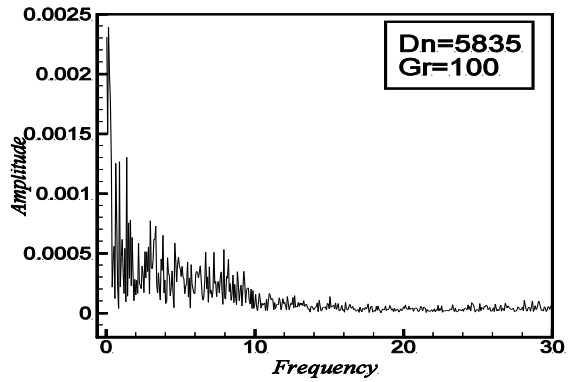


(b)

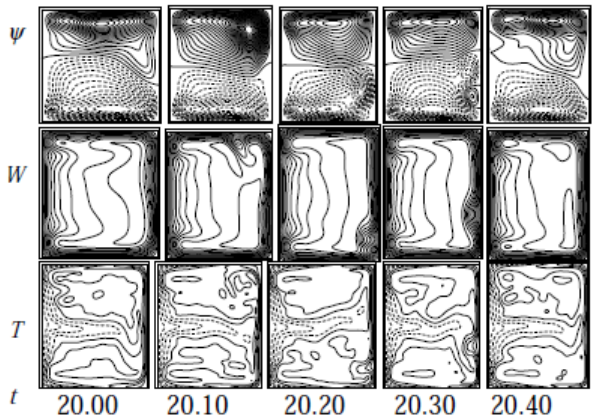


**(c)**

Fig. 10: **(a)** Time evolution of $\lambda$ for $Dn = 5835$ at time $16.10 \le t \le 21$ for $\delta = 0.5$ **; (b)** Power spectra of the time evolution of $\lambda$ for $Dn = 5835$ for $\delta = 0.5$ **; (c)** Contours of secondary flow, axial flow distribution and temperature profiles for $Dn = 5835$ at time $20.00 \le t \le 20.40$

## VI. Conclusions

In this present study, a detailed numerical study on the fully developed two-dimensional flow of viscous incompressible fluid through a curved channel with strong curvature has been performed by using the spectral method and covering a wide range of the Dean number $Dn$, $100 \le Dn \le 6000$ and the Grashof number $Gr = 100$ for the curvature $\delta = 0.5$. After a comprehensive survey over range of the parameters two branches of asymmetric steady solutions are obtained for $Dn$ lying in the range. Contours of typical secondary flow patterns, axial flow distribution and temperature profiles are also obtained at several values of the Dean number for the steady-state, periodic, multi-periodic and chaotic solutions.

For the unsteady solution we obtain two-, three- and four-vortex solutions. Then, in order to investigate the non-linear behavior of the unsteady solutions, time evaluations calculations as well as their spectral analysis are performed. It is found that the flow becomes steady-state for $Dn \le 4345$, periodic for $4350 \le Dn \le 4475$, multi-periodic solutions for $4500 \le Dn \le 5050$, and chaotic solutions for $5075 \le Dn \le 5835$. Thus the unsteady flow undergoes in the scenario "*steady* $\rightarrow$ *periodic* $\rightarrow$ *multi-periodic* $\rightarrow$ *chaotic*", if $Dn$ is increased up to 5835, i.e. $Dn \le 5835$. If the Dean number is increased further, that is, $Dn > 5840$ the unsteady flow undergoes through various flow instabilities, if $Dn$ is increased gradually. Thus, in order to investigate the transition from periodic to multi-periodic oscillation or the multi-periodic oscillation to chaotic state in more detail, the spectral analysis is found to be very useful. So, the transition of the unsteady solutions is clearly determined by the power spectrum of the solution.

## References

[1] Berger, S.A., Talbot, L., Yao, L. S. Flow in Curved Pipes. *Annual. Rev. Fluid. Mech*. 1983; **35**: 461-512.

[2] Dean, W. R. Note on the motion of fluid in a curved pipe. *Phil. Mag .1927;* **4** (20): 208- 223.

[3] Gottlieb, D. and Orazag, S. A. Numerical Analysis of Spectral Methods. *Society for Industrial and Applied Mathematics*: Philadelphia; 1977.

[4] Keller, H. B. Lectures on Numerical Methods in Bifurcation Problems. *Springer:* Berlin; 1987.

[5] Ito, H. Flow in Curved Pipes. *JSME Int. J*. 1987; **30:** 543-552.

[6] Mondal, R. N. Isothermal and Non-isothermal Flows through Curved ducts with Square and Rectangular Cross Sections. *Ph.D. Thesis*, Department of Mechanical Engineering, Okayama University: Japan; 2006.

[7] Mondal, R. N., Kaga, Y., Hyakutake, T. and Yanase, S. Bifurcation diagram for two-dimensional steady flow and unsteady solutions in a curved square duct. *Fluid Dynamics Research* 2007a; 39: 413-446.

 

[8] Mondal, R. N., Uddin, M. S. and Islam, A. Non-isothermal flow through a curved rectangular duct for large Grashof number. *J. Phy. Sci.* 2008; **12:** 109-121.

[9] Nandakumar, K. and Masliyah, J. H. Swirling Flow and Heat Transfer in Coiled and Twisted Pipes. *Adv. Transport Process* 1986; 4: 49-112.

[10] Wang, L. and Yang, T. Bifurcation and stability of forced convection in curved ducts of square cross section. *Int. journal of Heat Mass Transfer* 2004; 47: 971-2987.

[11] Yanase, S., Mondal, R.N., kaga, Y. and Yamamoto, K. Transition from steady to chaotic states of isothermal and non-isothermal flows through a curved rectangular duct. J. Phys. Soc. 2005; 74(1): 345-358.

[12] Winters, K. H. A Bifurcation Study of Laminar Flow in a Curved Tube of Rectangular Cross-section. *Journal of Fluid Mechanics* 1987; 180: 343-369.

[13] Yanase, S., Kaga, Y. and Daikai, R. Laminar flow through a curved rectangular duct over a wide range of the aspect ratio. *Fluid Dynamics Research 2002;* 31: 151-183

**Authors' Profiles**

**M. M. Rahman** was born in Bangladesh on 11th January, 1984. He received the B.Sc. (Honours) in Mathematics and M.Sc. in Applied Mathematics degrees from Khulna University. He is currently a Lecturer in the Department of Mathematics, Islamic University (IU), Kushtia, Bangladesh. His research directions include Numerical Analysis, Wavelet Analysis, Nonlinear Analysis, Statistical Analysis and Fluid Mechanics.

**M. A. Hye** was born in Bangladesh on 10th October, 1986. He received the B.Sc. in Mathematics and M. Sc in Applied Mathematics degrees from Khulna University. He is currently a Lecturer in the Department of Mathematics and Statistics, Bangladesh University of Business and Technology (BUBT). His research interests include Fluid Dynamics and Operation Research.

**How to cite this paper:** M. M. Rahman, M. A. Hye,"Non-isothermal Flow through a Curved Channel with Strong Curvature", International Journal of Intelligent Systems and Applications (IJISA), vol.5, no.9, pp.76-85, 2013. DOI: 10.5815/ijisa.2013.09.09

 